

Thermal neutron capture cross section for $^{56}\text{Fe}(n,\gamma)$ R. B. Firestone,^{1,2} T. Belgia,³ M. Krtička,⁴ F. Bečvář,⁴ L. Szentmiklósi,³ and I. Tomandl⁵¹*University of California, Department of Nuclear Engineering, Berkeley, California 94720, USA*²*Lawrence Berkeley National Laboratory, Berkeley, California 94720, USA*³*Centre for Energy Research, Hungarian Academy of Sciences, H-1525 Budapest, Hungary*⁴*Charles University in Prague, Faculty of Mathematics and Physics, V. Holešovičkách 2, CZ-180 00 Prague 8, Czech Republic*⁵*Nuclear Physics Institute, Czech Academy of Sciences, CZ-250 68 Řež, Czech Republic*

(Received 24 October 2016; published 30 January 2017)

The $^{56}\text{Fe}(n,\gamma)$ thermal neutron capture cross section and the ^{57}Fe level scheme populated by this reaction have been investigated in this work. Singles γ -ray spectra were measured with an isotopically enriched ^{56}Fe target using the guided cold neutron beam at the Budapest Reactor, and $\gamma\gamma$ -coincidence data were measured with a natural Fe target at the LWR-15 research reactor in Řež, Czech Republic. A detailed level scheme consisting of 448 γ rays populating/depopping 97 levels and the capture state in ^{57}Fe has been constructed, and $\approx 99\%$ of the total transition intensity has been placed. The transition probability of the 352-keV γ ray was determined to be $P_\gamma(352) = 11.90 \pm 0.07$ per 100 neutron captures. The ^{57}Fe level scheme is substantially revised from earlier work and ≈ 33 previously assigned levels could not be confirmed while a comparable number of new levels were added. The ^{57}Fe γ -ray cross sections were internally calibrated with respect to ^1H and ^{32}S γ -ray cross section standards using iron(III) acetylacetonate ($\text{C}_{15}\text{H}_{21}\text{FeO}_6$) and iron pyrite (FeS_2) targets. The thermal neutron cross section for production of the 352-keV γ -ray cross section was determined to be $\sigma_\gamma(352) = 0.2849 \pm 0.015$ b. The total $^{56}\text{Fe}(n,\gamma)$ thermal radiative neutron cross section is derived from the 352-keV γ -ray cross section and transition probability as $\sigma_0 = 2.394 \pm 0.019$ b. A least-squares fit of the γ rays to the level scheme gives the ^{57}Fe neutron separation energy $S_n = 7646.183 \pm 0.018$ keV.

DOI: [10.1103/PhysRevC.95.014328](https://doi.org/10.1103/PhysRevC.95.014328)**I. INTRODUCTION**

Precise thermal neutron capture γ -ray spectra were measured for all elements with $Z = 1-83, 90, \text{ and } 92$, except for He and Pm, using neutron beams at the Budapest Reactor [1,2]. The γ -ray energies and cross sections were determined and combined, together with additional information from the literature, to generate the Evaluated Gamma-ray Activation File (EGAF) [3] and they were also published in the *Handbook of Prompt Gamma Activation Analysis with Neutron Beams* [4]. These data can be used to determine total radiative thermal neutron capture cross sections, σ_0 . When the level scheme is complete, σ_0 equals both the sum of transition cross sections, γ -ray plus conversion electron, feeding the ground state (GS), $\Sigma\sigma_{\gamma+e}(\text{GS})$, and the sum of transition cross sections deexciting the capture state (CS), $\Sigma\sigma_{\gamma+e}(\text{CS})$. Thermal neutron capture decay schemes are typically completely determined for low- Z elements where all of the transitions are observed.

Iron is an important structural and shielding material in nuclear reactors and other nuclear installations that has an important impact on thermal neutron flux distribution in a reactor pressure vessel [5]. Despite its importance, the $^{56}\text{Fe}(n,\gamma)$ total radiative thermal neutron cross section, σ_0 , is only known to an accuracy of $\approx 5\%$ based on only two early measurements from over 40 years ago. In this work the $^{56}\text{Fe}(n,\gamma)$ reaction has been studied with a thermal equivalent neutron beam impinging on an enriched ^{56}Fe target. The corresponding ^{57}Fe γ -ray decay scheme has been nearly completely determined with only minor corrections necessary to account for the weak, missing, or unplaced γ -ray intensity. The new γ -ray data have been internally calibrated with thermal cross section γ -ray standards to determine a new value

of the total radiative thermal neutron cross section accurate to $\approx 0.8\%$.

The $^{56}\text{Fe}(n,\gamma)$ reaction was previously studied by Vennink *et al.* [6], who placed 191 γ rays that populated/depopped 62 levels in ^{57}Fe . Levels and γ rays were assigned by Vennink *et al.* on the basis of γ -ray energy sums but without the aid of $\gamma\gamma$ coincidence data. That procedure can be unreliable due to a high probability of chance energy sums matching known level energies resulting from the complexity of the (n,γ) spectrum. In this work we have also exploited $\gamma\gamma$ coincidence spectra, originally measured for studying two-step γ cascades [7] using a natural Fe target, to confirm the placement of more than 70% of the transitions observed in γ -ray singles measurements, add new transitions, and divide the intensities of γ rays that could be multiply placed in the decay scheme.

II. EXPERIMENT

The singles $^{56}\text{Fe}(n,\gamma)$ neutron capture γ -ray spectrum was measured in the guided cold neutron beam at the 10-MW Budapest Reactor [1]. Neutrons entered the evacuated target holder and continued to the beam stop at the rear wall of the guide hall. The target station, where both primary and secondary γ rays can be measured in low background conditions, is located 30 m from the reactor. The thermal-equivalent neutron flux at the target was $1.2 \times 10^8 \text{ cm}^{-2} \text{ s}^{-1}$ during this experiment.

Prompt γ rays from the target were measured with an n -type high-purity, 27% efficient, germanium (HPGe) detector with closed-end coaxial geometry located 23.5 cm from the target. The detector is Compton-suppressed by a bismuth germanate

TABLE I. $^{56}\text{Fe}(n, \gamma)$ thermal neutron capture γ ray energies and relative intensities measured in this work for γ energies from 14 to 352 keV, with detailed transition characteristics.

E_γ (keV)	I_γ^a	Multipolarity [12]	Mixing ratio δ [12]	ICC [13]	Placement (initial \rightarrow final)
14.4130(3) ^{b,c}	55.0(4)	$M1 + E2$	0.00223(1)	8.54(2)	14 \rightarrow 0
92(1) ^d	0.08(3)	[M1]		0.044(2)	7646 \rightarrow 7554
105.5(3)	0.051(17)				unplaced
119.86(11) ^e	0.172(25)	$M1$		0.0218(3)	3547 \rightarrow 3428
122.026(14) ^c	35.4(6)	$M1 + E2$	0.120(1)	0.0238(4)	136 \rightarrow 14
134.00(24)	0.046(12)				unplaced
136.441(16) ^c	4.51(8)	$E2$		0.149(2)	136 \rightarrow 0
186.7(4) ^e	0.020(10)	[M1]		0.007(1)	5495 \rightarrow 5308
200.60(21)	0.068(13)				unplaced
204.52(24)	0.064(13)				unplaced
230.298(13) ^c	9.70(14)	[M1]		0.0042(1)	367 \rightarrow 136
318.96(6) ^e	0.131(11)	[M1]		0.00190(3)	3240 \rightarrow 2921
325(1) ^d	0.5(2)	[M1]		0.00181(3)	7646 \rightarrow 7321
333(1) ^c	0.22(8)	[M1]		0.00171(3)	7646 \rightarrow 7313
339.618(14) ^f	1.61(3)	[M1]		0.00164(2)	706 \rightarrow 367
350(1) ^g	0.29(10)	[M1]		0.00152(2)	1357 \rightarrow 1007
352.347(13) ^c	100.0(14)	$M1 + E2$	0.025(9)	0.0029(15)	367 \rightarrow 14

^aRelative intensity. For multiply placed transitions the singles γ -ray intensity has been divided on the basis of intensity balance and coincidence data. Multiply by 0.1190(7) for transition probability per 100 neutron captures, $P_\gamma(\%)$.

^bNot observed. Intensity calculated from intensity balance feeding the 14.4-keV level and corrected for unobserved continuum feeding (see text).

^cTransition confirmed by coincidence data.

^dExpected primary γ -ray transition, see text.

^eTransition placed by energy sums.

^fTransition adopted from ENSDF [12].

^gTransition proposed from intensity balance but likely obscured by strong 352-keV γ -ray.

(BGO) scintillator guard detector annulus surrounded by 10-cm-thick lead shielding. Relative detection efficiency was calibrated from 50 keV to 10 MeV with radioactive sources and (n, γ) reaction γ rays to a precision of better than 1% from 500 keV to 6 MeV and better than 2% at 100–500 keV and >6 MeV [8]. The γ -ray spectra were analyzed using the HYPERMET PC program [8,9].

An FeO target enriched to 99.94% in ^{56}Fe , suspended in a Teflon bag to minimize background from the target holder, was irradiated to obtain a high statistics, impurity free ^{57}Fe spectrum. No target impurity γ rays were observed in the prompt γ -ray spectrum, verifying that nearly all of the observed γ rays could be assigned to ^{57}Fe . Elemental radiative thermal neutron γ -ray cross sections were normalized, with respect to hydrogen and sulfur standard γ rays, using stoichiometric high purity iron(III) acetylacetonate ($\text{C}_{15}\text{H}_{21}\text{FeO}_6$) and iron pyrite (FeS_2) targets where the isotopic cross sections were determined from the ^{56}Fe natural abundance [10].

Coincidence data were measured at the LWR-15 research reactor in Řež with two HPGe detectors, with efficiencies of 20% and 25% respectively, placed above and below the horizontally situated target with their axes parallel to each other. Sum coincidence gates were set on γ rays deexciting the capture state and populating levels at 0, 14, 136, 367, 706, 1265, 1627, 1725, 2118, and 2207 keV in ^{57}Fe via two-step cascades. The two-step coincidence method is described in detail by Honzátko *et al.* [11].

III. ^{57}Fe DECAY SCHEME

A total of 472 γ -ray transitions, including numerous unresolved multiplets, were assigned to the $^{56}\text{Fe}(n, \gamma)$ reaction and 448 γ -rays were placed in the ^{57}Fe level scheme; they are summarized in Tables I and II. The low energy 14.4-keV transition connecting the first excited and ground states was not observed in this work, and its intensity has been inferred from the total intensity feeding the 14.4-keV level. Most transition placements were confirmed by the sum coincidence data. Other γ rays were previously placed on the basis of previous work in the Evaluated Nuclear Structure Data File (ENSDF) evaluation [12]. Some γ rays were placed on the basis of energy sums and intensity balance considerations. The intensities of the unresolved multiplets were divided on the basis of coincidence data and the decay scheme intensity balance. The 92-, 325-, and 333-keV primary γ rays were too weak to be observed but are assumed to exist because they feed levels that are too high in excitation energy to be significantly populated by other weakly fed, higher-lying states. The γ -rays at 7313 and 7554 keV are arbitrarily assumed to populate the GS. They are too weak to be observed in the coincidence data. The level at 7321 keV was placed on the basis that the 7306.5-keV transition is very weakly observed in sum coincidence with the 14-keV level, and a 1346.58-keV γ ray can be placed deexciting this level to the 5975-keV level on the basis of energy sums. Expected $E1$ primary γ rays populating the 2554.12-, 2574.07-, and

TABLE II. $^{56}\text{Fe}(n, \gamma)$ thermal neutron capture γ ray energies and relative intensities measured in this work for γ energies of 366 keV and higher.

E_γ (keV)	I_γ^a	Placement (initial \rightarrow final)
366.752(13) ^b	18.03(25)	367 \rightarrow 0
460.42(7) ^b	0.685(23)	1725 \rightarrow 1265
487.9(4)	0.013(9)	unplaced
490.92(11) ^b	0.061(14)	2118 \rightarrow 1627
525.91(10) ^b	0.063(12)	7646 \rightarrow 7120
566.4(3) ^c	0.024(8)	4548 \rightarrow 3982
569.966(15) ^d	4.78(7)	706 \rightarrow 136
628.59(9) ^b	0.112(11)	2836 \rightarrow 2207
635.33(8) ^c	0.104(11)	6676 \rightarrow 6040
640.50(18) ^d	0.051(11)	1007 \rightarrow 367
650.70(3) ^d	1.71(3)	1357 \rightarrow 706
665.66(7) ^c	0.184(18)	3240 \rightarrow 2574
689.8(5) ^c	0.16(4)	5238 \rightarrow 4548
692.005(14) ^b	50.9(7)	706 \rightarrow 14
706.42(4) ^b	2.14(4)	706 \rightarrow 0
717.9(4) ^b	0.070(17)	2836 \rightarrow 2118
731.07(10) ^c	0.179(16)	6160 \rightarrow 5429
734.90(8) ^d	0.617(23)	3240 \rightarrow 2505
746.49(12)	0.082(21)	unplaced
761.10(4) ^c	0.273(19)	2118 \rightarrow 1357
779.68(14) ^b	0.063(9)	2505 \rightarrow 1725
809(1) ^b	0.44(15)	7646 \rightarrow 6837
821.04(6) ^c	0.171(15)	3792 \rightarrow 2971
834.9(5) ^c	0.014(13)	5084 \rightarrow 4249
849.7(4) ^c	0.050(14)	3547 \rightarrow 2697
853.0(6) ^c	0.024(13)	3428 \rightarrow 2574
855.89(17) ^b	0.095(15)	7646 \rightarrow 6790
867.82(22) ^b	0.086(19)	7646 \rightarrow 6778
870.68(8) ^d	1.21(4)	1007 \rightarrow 136
873.2(4) ^c	0.047(15)	3428 \rightarrow 2554
877.0(3) ^c	0.083(15)	4249 \rightarrow 3371
894.1(4)	0.060(15)	unplaced
898.251(15) ^b	19.4(3)	1265 \rightarrow 367
900.68(6) ^b	0.324(20)	7646 \rightarrow 6746
911.67(20) ^c	0.055(13)	4209 \rightarrow 3298
920.843(15) ^b	7.71(11)	1627 \rightarrow 706
922(1) ^b	0.12(6)	7646 \rightarrow 6724
950.2(3) ^c	0.035(13)	4249 \rightarrow 3298
955.79(11) ^c	0.115(17)	3792 \rightarrow 2836
970.48(12) ^b	0.144(19)	7646 \rightarrow 6676
987.52(20)	0.063(16)	unplaced
990.42(11) ^d	0.574(22)	1357 \rightarrow 367
992.85(10) ^b	0.671(25)	1007 \rightarrow 14
994.7(3) ^b	0.19(3)	7646 \rightarrow 6652
998.0(6) ^c	0.019(13)	5689 \rightarrow 4692
1007.09(10) ^b	0.117(12)	4379 \rightarrow 3371
1014.11(19)	0.099(13)	unplaced
1016.2(3)	0.12(3)	unplaced
1018.983(19) ^b	18.28(25)	1725 \rightarrow 706
1021.93(18) ^b	0.077(12)	7646 \rightarrow 6624
1028.5(3) ^c	0.43(13)	6075 \rightarrow 5046
1030.73(20)	0.084(14)	unplaced
1032.66(21) ^b	0.073(14)	3240 \rightarrow 2207
1056.9(3) ^c	0.027(13)	6365 \rightarrow 5308

TABLE II. (Continued.)

E_γ (keV)	I_γ^a	Placement (initial \rightarrow final)
1062.05(24) ^d	0.056(13)	1198 \rightarrow 136
1069.98(13) ^c	0.089(13)	2697 \rightarrow 1627
1094.53(6) ^c	0.328(18)	3792 \rightarrow 2697
1099.6(5) ^c	0.230(18)	6408 \rightarrow 5308
1102.24(23) ^c	0.092(15)	5084 \rightarrow 3982
1110.95(3) ^b	7.7(3)	2836 \rightarrow 1725
1130.49(6) ^b	0.216(16)	7646 \rightarrow 6516
1162.36(22) ^c	0.061(11)	4460 \rightarrow 3298
1164.4(5) ^b	0.171(15)	3371 \rightarrow 2207
1165(1) ^b	0.06(3)	7646 \rightarrow 6481
1193.6(3) ^c	0.068(20)	5886 \rightarrow 4692
1196.87(4) ^c	2.15(4)	2554 \rightarrow 1357
1200.04(4) ^d	0.789(24)	2207 \rightarrow 1007
1208.70(12) ^b	0.169(16)	2836 \rightarrow 1627
1217.61(5) ^c	0.557(21)	3792 \rightarrow 2574
1221.54(15) ^b	0.141(16)	3428 \rightarrow 2207
1237.55(6) ^b	0.87(6)	7646 \rightarrow 6408
1238.73(15) ^c	0.31(6)	4209 \rightarrow 2971
1250.68(3) ^b	1.14(3)	1265 \rightarrow 14
1253.9(3) ^c	0.067(16)	6746 \rightarrow 5492
1256.83(20) ^c	0.104(17)	5238 \rightarrow 3982
1260.535(21) ^b	25.2(3)	1627 \rightarrow 367
1264.96(5) ^b	0.403(18)	1265 \rightarrow 0
1268.38(19) ^c	0.090(18)	6314 \rightarrow 5046
1277.15(11) ^c	0.125(15)	4460 \rightarrow 3183
1281.31(4) ^b	0.851(23)	7646 \rightarrow 6365
1284.0(5) ^d	0.5(2)	3982 \rightarrow 2697
1288.61(20) ^c	0.065(13)	4209 \rightarrow 2921
1293.32(4) ^b	0.299(25)	2921 \rightarrow 1627
	1.09(3)	7646 \rightarrow 6353
1300.06(17) ^b	0.110(14)	7646 \rightarrow 6346
1309.77(17) ^b	0.078(14)	3428 \rightarrow 2118
1324.96(24) ^c	0.078(15)	6408 \rightarrow 5084
1328.0(3) ^c	0.048(14)	4249 \rightarrow 2921
1332.34(8) ^b	0.317(17)	7646 \rightarrow 6314
1342.78(7) ^d	0.682(22)	1357 \rightarrow 14
1346.58(10) ^c	0.206(17)	7321 \rightarrow 5975
1358.679(22) ^b	7.91(12)	1725 \rightarrow 367
1361.6(3) ^b	0.079(20)	7646 \rightarrow 6285
1364.69(6) ^c	0.344(19)	4548 \rightarrow 3183
1373.5(3) ^c	0.050(17)	4209 \rightarrow 2836
1380.46(18) ^c	0.116(19)	5629 \rightarrow 4249
1407.72(5) ^c	0.345(14)	4379 \rightarrow 2971
1411.85(4) ^d	2.02(3)	2118 \rightarrow 706
1430.74(11) ^b	0.407(19)	7646 \rightarrow 6215
1433.9(5) ^c	0.103(15)	5894 \rightarrow 4460
1450.75(19)	0.092(15)	unplaced
1457.79(12) ^b	0.343(24)	3183 \rightarrow 1725
1463.14(19) ^c	0.087(17)	5924 \rightarrow 4460
1486.75(11) ^b	0.59(3)	7646 \rightarrow 6160
1490.75(13) ^b	1.21(3)	1627 \rightarrow 136
1511.49(2)	0.07(3)	unplaced
1513.9(5) ^b	0.34(3)	3240 \rightarrow 1725
1529.15(11) ^c	0.167(16)	6837 \rightarrow 5308
	0.167(16)	7646 \rightarrow 6117

TABLE II. (*Continued.*)TABLE II. (*Continued.*)

E_γ (keV)	I_γ^a	Placement (initial \rightarrow final)
1542.18(19) ^b	0.088(16)	3660 \rightarrow 2118
1549.36(19) ^c	0.100(16)	5689 \rightarrow 4140
1555.70(8) ^b	0.185(17)	3183 \rightarrow 1627
1571.02(4) ^b	0.513(23)	7646 \rightarrow 6075
	0.13(3)	2836 \rightarrow 1265
1574.34(21)	0.103(16)	unplaced
1582.82(22) ^c	0.104(23)	6408 \rightarrow 4826
1584.60(3) ^b	0.21(3)	3792 \rightarrow 2207
	0.85(3)	7646 \rightarrow 6061
1589.05(3) ^b	0.668(19)	1725 \rightarrow 136
1599.09(16) ^c	0.105(14)	6837 \rightarrow 5238
1605.8(3) ^c	0.102(14)	7646 \rightarrow 6040
1608.81(17) ^b	0.136(17)	7646 \rightarrow 6037
	0.042(17)	5429 \rightarrow 3820
1612.918(18) ^b	54.21(13)	1627 \rightarrow 14
	0.41(9)	2971 \rightarrow 1357
	1.25(13)	3240 \rightarrow 1627
1616.82(16) ^b	0.114(16)	7646 \rightarrow 6029
1624.28(21) ^c	0.111(20)	4460 \rightarrow 2836
1627.34(4) ^b	3.33(6)	1627 \rightarrow 0
1633.4(3) ^b	0.104(25)	7646 \rightarrow 6013
1635.26(5) ^c	0.98(3)	4209 \rightarrow 2574
1646.2(5) ^b	0.384(17)	3371 \rightarrow 1725
1655.44(4) ^d	0.402(16)	2921 \rightarrow 1265
	1.06(3)	4209 \rightarrow 2554
1662.6(3) ^c	0.047(14)	4845 \rightarrow 3183
1671.49(6) ^b	0.361(16)	7646 \rightarrow 5975
1681.96(15) ^d	0.104(14)	4379 \rightarrow 2697
1692.89(9)	0.148(17)	unplaced
1702.35(7) ^b	0.390(18)	3428 \rightarrow 1725
1704.8(5) ^d	0.197(17)	4209 \rightarrow 2505
1711.09(3) ^b	1.16(3)	1725 \rightarrow 14
1721.1(3) ^c	0.27(10)	4692 \rightarrow 2971
1722.65(4) ^b	3.89(9)	7646 \rightarrow 5924
1725.459(18) ^b	64.1(9)	1725 \rightarrow 0
1736.68(23)	0.095(16)	unplaced
1743.85(6) ^b	0.368(18)	3371 \rightarrow 1627
1752.64(8) ^b	0.228(16)	7646 \rightarrow 5894
1760.06(3) ^b	0.885(23)	7646 \rightarrow 5886
1798.85(12) ^b	0.164(16)	2505 \rightarrow 706
1824.26(14) ^c	0.154(16)	4379 \rightarrow 2554
1840.62(5) ^d	0.592(22)	2207 \rightarrow 367
1847.70(14) ^c	0.147(16)	2554 \rightarrow 706
1851.78(4) ^c	0.580(21)	4773 \rightarrow 2921
1856.04(4) ^b	0.671(23)	7646 \rightarrow 5790
1863.18(21) ^c	0.088(16)	3982 \rightarrow 2118
1867.76(25) ^c	0.069(15)	2574 \rightarrow 706
1874.28(23) ^c	0.065(14)	4845 \rightarrow 2971
1886.15(6) ^c	0.318(20)	4460 \rightarrow 2574
1894.2(3)	0.056(19)	unplaced
1900.4(3) ^c	0.058(18)	6746 \rightarrow 4845
1906.05(5) ^c	0.434(23)	4460 \rightarrow 2554
1932.92(16) ^b	0.125(20)	7646 \rightarrow 5713
1944.02(21) ^c	0.118(18)	5492 \rightarrow 3547
1951.83(20) ^b	0.122(17)	4159 \rightarrow 2207

E_γ (keV)	I_γ^a	Placement (initial \rightarrow final)
1956.81(14) ^b	0.54(3)	7646 \rightarrow 5689
1974.88(3) ^b	0.97(3)	3240 \rightarrow 1265
1981.78(13) ^c	0.137(15)	2118 \rightarrow 136
1991(1) ^b	0.16(6)	2697 \rightarrow 706
2002.21(5) ^b	2.00(4)	4209 \rightarrow 2207
2016.94(6) ^b	0.568(22)	7646 \rightarrow 5629
2066.29(4) ^b	4.65(8)	3792 \rightarrow 1725
2070.77(6) ^c	0.69(3)	2207 \rightarrow 136
2075.64(12) ^c	0.171(24)	4773 \rightarrow 2697
2091.18(5) ^b	2.05(4)	4209 \rightarrow 2118
2103.83(6) ^d	0.79(3)	2118 \rightarrow 14
2106.06(19) ^b	0.182(20)	3371 \rightarrow 1265
2124.4(3) ^b	0.086(18)	7646 \rightarrow 5522
2129.464(23) ^b	7.42(11)	2836 \rightarrow 706
2138.19(3) ^b	2.40(5)	2505 \rightarrow 367
2151.61(3) ^b	2.06(4)	7646 \rightarrow 5495
2154.59(10) ^b	0.353(22)	7646 \rightarrow 5492
2157.81(14) ^c	0.175(19)	7646 \rightarrow 5488
2165(1) ^b	0.030(15)	7646 \rightarrow 5482
2171.10(6) ^b	0.383(21)	4379 \rightarrow 2207
2187.17(7) ^c	0.622(20)	4692 \rightarrow 2505
2192.78(7) ^d	1.73(3)	2207 \rightarrow 14
2197.7(4) ^c	0.036(15)	6746 \rightarrow 4548
2207.36(10) ^b	0.48(3)	2207 \rightarrow 0
	0.30(3)	2574 \rightarrow 367
2209.90(16) ^c	0.03(3)	5046 \rightarrow 2836
2217.26(11) ^b	0.278(22)	7646 \rightarrow 5429
2254.60(17) ^c	0.174(22)	5495 \rightarrow 3240
2260.18(8) ^b	0.415(25)	4379 \rightarrow 2118
2264.28(5) ^b	0.67(3)	2971 \rightarrow 706
2308.4(5) ^c	0.079(23)	5492 \rightarrow 3183
2330.23(4) ^b	0.72(3)	2697 \rightarrow 367
2338.04(6) ^b	0.315(20)	7646 \rightarrow 5308
2354.6(3) ^b	0.055(18)	3982 \rightarrow 1627
2361.77(20)	0.139(18)	unplaced
2368.42(4) ^b	0.726(25)	2505 \rightarrow 136
2385.824(25) ^b	1.32(3)	7646 \rightarrow 5260
2403.8(6) ^c	0.087(23)	6652 \rightarrow 4249
2407.79(5) ^b	1.33(4)	7646 \rightarrow 5238
2414.58(17) ^b	0.190(25)	4140 \rightarrow 1725
2419.2(5)	0.035(22)	5790 \rightarrow 3371
2424.16(5) ^c	1.01(3)	5260 \rightarrow 2836
	0.51(3)	7646 \rightarrow 5222
2433.72(14) ^b	0.26(3)	4159 \rightarrow 1725
2437.53(13) ^c	0.25(3)	2574 \rightarrow 136
2450.3(9) ^c	0.054(25)	5689 \rightarrow 3240
2457.55(19) ^b	0.15(3)	4575 \rightarrow 2118
2462.53(11) ^c	0.304(25)	3820 \rightarrow 1357
2469.10(4) ^b	3.55(7)	2836 \rightarrow 367
2472.3(3) ^c	0.11(3)	5308 \rightarrow 2836
2477.7(10) ^b	0.14(3)	3183 \rightarrow 706
2481(1) ^b	0.16(8)	7646 \rightarrow 5164
2484.65(7) ^b	0.28(3)	4209 \rightarrow 1725
	0.28(3)	4692 \rightarrow 2207
2508.22(13) ^c	0.222(20)	5429 \rightarrow 2921

TABLE II. (*Continued.*)

E_γ (keV)	I_γ^a	Placement (initial \rightarrow final)
2526.678(18) ^b	4.22(7)	3792 \rightarrow 1265
2532(1) ^b	0.25(12)	4159 \rightarrow 1627
2540.02(19) ^c	0.121(19)	3547 \rightarrow 1007
2553.56(16) ^b	0.140(20)	2554 \rightarrow 0
2562.53(11) ^b	0.41(4)	7646 \rightarrow 5084
	0.16(4)	2697 \rightarrow 136
2573.980(25) ^d	1.70(4)	2574 \rightarrow 0
2582.06(4) ^b	0.85(3)	4209 \rightarrow 1627
2600.00(14) ^b	0.189(20)	7646 \rightarrow 5046
2603.88(4) ^b	0.78(3)	2971 \rightarrow 367
2653.10(7) ^b	0.83(5)	4379 \rightarrow 1725
2655.5(4) ^b	0.16(4)	4773 \rightarrow 2118
2658.7(3) ^c	0.095(23)	5629 \rightarrow 2971
2664.30(23) ^b	0.12(3)	3371 \rightarrow 706
2682.599(18) ^b	4.30(7)	2697 \rightarrow 14
	0.25(8)	7646 \rightarrow 4964
2686.20(10) ^c	0.268(19)	5260 \rightarrow 2574
2692.44(6) ^d	0.458(20)	6353 \rightarrow 3660
2697.02(3) ^b	3.11(6)	2697 \rightarrow 0
2699.50(10) ^b	0.55(4)	2836 \rightarrow 136
2715.7(3) ^b	0.19(3)	4923 \rightarrow 2207
2721.365(22) ^b	14.8(6)	3428 \rightarrow 706
2724(1) ^b	0.34(11)	7646 \rightarrow 4923
2734.72(4) ^b	1.59(7)	4460 \rightarrow 1725
2751.05(4) ^b	1.43(6)	4379 \rightarrow 1627
2766.44(19) ^c	0.18(3)	6314 \rightarrow 3547
2800.62(6) ^b	0.81(4)	7646 \rightarrow 4845
2813.77(7) ^b	1.06(5)	7646 \rightarrow 4832
2816.1(5) ^b	0.12(5)	3183 \rightarrow 367
2821.88(6) ^b	0.82(3)	7646 \rightarrow 4826
2833.01(5) ^b	2.38(12)	4460 \rightarrow 1627
2834.2(5) ^b	1.34(16)	2971 \rightarrow 136
2835.9(5) ^b	5.42(10)	2836 \rightarrow 0
2840.9(3) ^b	0.13(3)	3547 \rightarrow 706
2849.9(3) ^b	0.14(3)	4575 \rightarrow 1725
2873.49(4) ^b	3.79(7)	7646 \rightarrow 4773
2894.12(11) ^b	0.296(22)	4159 \rightarrow 1265
2905.96(18) ^b	0.217(23)	2921 \rightarrow 14
2920.93(12) ^b	0.30(3)	2921 \rightarrow 0
2944.48(8) ^b	0.78(3)	4209 \rightarrow 1265
2953.97(7) ^b	0.19(9)	3660 \rightarrow 706
	3.12(12)	7646 \rightarrow 4692
2956.18(14) ^b	0.74(9)	2971 \rightarrow 14
2966.83(21) ^b	0.37(4)	4692 \rightarrow 1725
2970.29(7) ^b	1.54(7)	2971 \rightarrow 0
3003.7(4) ^b	0.08(3)	3371 \rightarrow 367
3047.4(3) ^b	0.11(3)	3183 \rightarrow 136
3050.6(4) ^c	0.07(3)	4249 \rightarrow 1198
3061.06(3) ^b	1.65(4)	3428 \rightarrow 367
3070.85(6) ^b	0.89(3)	7646 \rightarrow 4576
3074.6(6) ^c	0.063(23)	5629 \rightarrow 2554
3095.2(3)	0.129(24)	unplaced
3098.38(16) ^b	0.34(3)	7646 \rightarrow 4548
3103.38(4) ^b	6.63(12)	3240 \rightarrow 136
3113.36(7) ^b	0.81(4)	4379 \rightarrow 1265

TABLE II. (*Continued.*)

E_γ (keV)	I_γ^a	Placement (initial \rightarrow final)
3146.3(4)	0.047(22)	unplaced
3164.02(14)	0.29(3)	unplaced
3168.58(5) ^b	4.09(8)	3183 \rightarrow 14
3172(1) ^b	0.22(11)	7646 \rightarrow 4474
3182.7(3) ^c	0.29(9)	3183 \rightarrow 0
3185.95(4) ^b	7.25(14)	7646 \rightarrow 4460
3225.41(6) ^b	3.60(7)	3240 \rightarrow 14
3234.4(3) ^b	0.184(25)	3371 \rightarrow 136
3239.82(4) ^b	3.25(7)	3240 \rightarrow 0
3267.43(4) ^b	13.33(22)	7646 \rightarrow 4379
3275.4(5)	0.06(3)	unplaced
3283.71(11) ^b	0.46(3)	3298 \rightarrow 14
3291.26(4) ^b	3.28(7)	3428 \rightarrow 136
3298.16(11) ^b	0.45(3)	3298 \rightarrow 0
3356.65(3) ^b	3.40(6)	3371 \rightarrow 14
3371.21(7) ^b	0.23(3)	3371 \rightarrow 0
	0.35(3)	4379 \rightarrow 1007
3397.78(25) ^b	0.154(23)	7646 \rightarrow 4249
3411(1) ^b	0.053(12)	3547 \rightarrow 136
3413.321(25) ^b	16.9(3)	3428 \rightarrow 14
3425(1) ^b	0.19(9)	3792 \rightarrow 367
3427.58(21) ^b	0.23(3)	3428 \rightarrow 0
3436.77(3) ^b	17.4(3)	7646 \rightarrow 4209
3444.32(20) ^c	0.21(3)	6365 \rightarrow 2921
3452.84(8) ^b	0.60(3)	3820 \rightarrow 367
3486.92(5) ^b	4.24(9)	7646 \rightarrow 4159
3502.70(5) ^b	1.95(5)	4209 \rightarrow 706
3507.45(5) ^b	1.74(6)	4773 \rightarrow 1265
	0.25(6)	7646 \rightarrow 4140
3513.0(3) ^b	0.13(3)	5238 \rightarrow 1725
3523.7(4) ^c	0.10(3)	3660 \rightarrow 136
3533.2(3) ^b	0.11(3)	3547 \rightarrow 14
3581.4(3) ^b	0.18(4)	3948 \rightarrow 367
3612.0(5) ^c	0.11(3)	6117 \rightarrow 2505
3615.03(13) ^b	0.40(3)	3982 \rightarrow 367
3633.11(11) ^b	0.39(3)	5260 \rightarrow 1627
3645.8(7) ^c	0.072(24)	3660 \rightarrow 14
3654.2(3) ^c	0.043(24)	6160 \rightarrow 2505
3664.38(5) ^b	1.32(4)	7646 \rightarrow 3982
3671.9(3) ^b	0.137(25)	4379 \rightarrow 706
3684.0(5) ^b	0.049(25)	3820 \rightarrow 136
3697.57(17) ^b	0.28(3)	7646 \rightarrow 3948
3710.9(3) ^c	0.35(4)	6408 \rightarrow 2697
3753.57(19) ^b	0.214(25)	4460 \rightarrow 706
3766.5(6) ^c	0.18(3)	5492 \rightarrow 1725
3772.4(3) ^b	0.150(24)	4140 \rightarrow 367
3777.26(4) ^b	2.83(6)	3792 \rightarrow 14
3792.32(4) ^b	2.18(5)	4159 \rightarrow 367
	0.03(1)	3792 \rightarrow 0
3805.0(3) ^b	0.116(24)	5924 \rightarrow 2118
3826.04(6) ^b	0.78(3)	7646 \rightarrow 3820
3842.48(4) ^b	3.04(6)	4209 \rightarrow 367
3845(1) ^b	0.06(3)	3982 \rightarrow 136
3854.36(3) ^b	13.22(21)	7646 \rightarrow 3792
3934.4(4) ^b	0.10(3)	3948 \rightarrow 14

TABLE II. (*Continued.*)

E_γ (keV)	I_γ^a	Placement (initial \rightarrow final)
3956.77(12) ^b	0.52(3)	5222 \rightarrow 1265
3962.6(5)	0.11(3)	unplaced
3967.3(3) ^b	0.25(3)	3982 \rightarrow 14
3981.50(14) ^b	0.49(4)	3982 \rightarrow 0
3985.3(4) ^b	0.31(3)	7646 \rightarrow 3660
3995.3(4) ^b	0.12(3)	5260 \rightarrow 1265
4011.9(3) ^b	4.19(8)	4379 \rightarrow 367
4072.69(9) ^b	1.96(5)	4209 \rightarrow 136
4093.47(19) ^b	0.31(3)	4460 \rightarrow 367
4098.68(16) ^b	0.34(3)	7646 \rightarrow 3547
4107(1) ^b	0.22(11)	4474 \rightarrow 367
4111.8(6) ^b	0.09(3)	4249 \rightarrow 136
4125.34(20) ^b	0.24(3)	4832 \rightarrow 706
4145(1) ^b	0.09(3)	4159 \rightarrow 14
4159.02(11) ^b	0.86(4)	4159 \rightarrow 0
4194.71(7) ^b	0.85(4)	4209 \rightarrow 14
4209.44(18) ^b	0.34(4)	4209 \rightarrow 0
4218.19(4) ^b	36.9(6)	7646 \rightarrow 3428
4242(1) ^b	0.10(3)	4379 \rightarrow 136
4259.3(5) ^b	0.082(24)	5886 \rightarrow 1627
4274.84(4) ^b	4.77(9)	7646 \rightarrow 3371
4300.61(4) ^c	0.35(4)	5308 \rightarrow 1007
4324.69(9) ^b	0.40(3)	4460 \rightarrow 136
	0.21(3)	4692 \rightarrow 367
4347.55(10) ^b	0.58(3)	7646 \rightarrow 3298
4364.4(3) ^b	1.00(4)	4379 \rightarrow 14
4378.69(6) ^b	2.35(6)	4379 \rightarrow 0
4406.09(4) ^b	0.44(15)	4773 \rightarrow 367
	16.3(3)	7646 \rightarrow 3240
4411.1(8) ^c	0.12(4)	4548 \rightarrow 136
4445.48(20) ^b	0.38(4)	4460 \rightarrow 14
4458.79(20) ^b	1.06(10)	4824 \rightarrow 367
4462.60(6) ^b	4.33(20)	7646 \rightarrow 3183
	1.0(3)	4460 \rightarrow 0
4531.9(3) ^b	0.44(3)	5238 \rightarrow 706
4548(1) ^b	0.19(9)	4548 \rightarrow 0
4555.6(3) ^b	0.99(5)	4692 \rightarrow 136
4560.2(4) ^b	0.25(3)	4575 \rightarrow 14
4575(1) ^b	0.13(3)	4575 \rightarrow 0
4588.1(5) ^c	0.09(3)	6215 \rightarrow 1627
4597(1) ^b	0.25(12)	4963 \rightarrow 367
4639.41(25) ^b	0.25(3)	6365 \rightarrow 1725
4658.52(9) ^b	0.83(4)	5924 \rightarrow 1265
4675.29(6) ^b	4.22(8)	7646 \rightarrow 2971
4679(1) ^b	0.10(5)	5046 \rightarrow 367
4694.8(4) ^b	0.15(3)	4832 \rightarrow 136
4725.69(24) ^b	0.17(3)	6353 \rightarrow 1627
4772.49(12) ^b	0.60(4)	4773 \rightarrow 0
4802.5(6) ^c	0.11(3)	6160 \rightarrow 1357
4809.94(5) ^b	16.1(3)	7646 \rightarrow 2836
4832.05(17) ^b	0.33(3)	4832 \rightarrow 0
4845.21(14) ^b	0.41(3)	4845 \rightarrow 0
4909(1) ^b	0.28(9)	4923 \rightarrow 14
4923.1(6) ^c	0.13(3)	4923 \rightarrow 0
4940.8(3) ^b	0.23(4)	5308 \rightarrow 367

TABLE II. (*Continued.*)

E_γ (keV)	I_γ^a	Placement (initial \rightarrow final)
4948.81(9) ^b	7.32(13)	7646 \rightarrow 2697
5069.2(3) ^b	0.26(5)	5084 \rightarrow 14
5083(1) ^b	0.13(3)	5084 \rightarrow 0
5100.6(4) ^b	0.13(4)	5238 \rightarrow 136
5125(1) ^b	0.12(3)	5492 \rightarrow 367
5127.2(6) ^b	0.14(5)	5495 \rightarrow 367
5140.9(3) ^b	1.61(6)	7646 \rightarrow 2505
5164(1) ^b	0.16(8)	5165 \rightarrow 0
5179.46(21) ^b	0.34(4)	5886 \rightarrow 706
5216.88(15) ^b	0.35(3)	5924 \rightarrow 706
5223.66(21) ^b	0.27(3)	5238 \rightarrow 14
5357.72(19) ^b	1.20(5)	5495 \rightarrow 136
5429.1(4) ^b	0.19(4)	5429 \rightarrow 0
5482(1) ^b	0.31(15)	5482 \rightarrow 0
5488(1) ^b	0.17(3)	5488 \rightarrow 0
5493.0(5) ^b	0.08(3)	5495 \rightarrow 0
	0.18(4)	5629 \rightarrow 136
5507.1(3) ^b	0.09(3)	5522 \rightarrow 14
5525.2(9) ^c	0.07(5)	6790 \rightarrow 1265
5553(1) ^b	0.07(2)	5689 \rightarrow 136
5615(1) ^b	0.03(1)	5629 \rightarrow 14
5646(1) ^b	0.09(3)	6013 \rightarrow 367
5653.4(3) ^b	0.41(6)	5789 \rightarrow 136
5673.3(5) ^c	0.38(6)	6040 \rightarrow 367
5698.8(12) ^b	0.07(6)	5713 \rightarrow 14
5749.5(3) ^b	0.19(4)	5886 \rightarrow 136
5776(1) ^b	0.4(2)	5789 \rightarrow 14
5786.76(10) ^b	0.88(5)	5924 \rightarrow 136
5838.2(4) ^b	0.18(5)	5975 \rightarrow 136
5886(1) ^b	0.24(8)	5886 \rightarrow 0
5893(1) ^b	0.05(2)	5894 \rightarrow 0
5909.7(8) ^b	0.22(6)	5924 \rightarrow 14
5920.20(5) ^b	80.7(16)	7646 \rightarrow 1725
5922.7(3) ^b	1.3(5)	5924 \rightarrow 0
5998.0(7) ^b	0.14(5)	6013 \rightarrow 14
6018.43(5) ^b	82.4(13)	7646 \rightarrow 1627
6029(1) ^b	0.12(3)	6029 \rightarrow 0
6037(1) ^b	0.16(8)	6038 \rightarrow 0
6046.9(3) ^b	0.24(4)	6062 \rightarrow 14
6061.07(15) ^b	0.61(5)	6062 \rightarrow 0
6073.8(7) ^b	0.12(4)	6075 \rightarrow 0
6103(1) ^b	0.12(6)	6117 \rightarrow 14
6117(1) ^b	0.21(3)	6117 \rightarrow 0
6144.7(3) ^b	0.28(5)	6160 \rightarrow 14
6200.5(4) ^b	0.31(6)	6215 \rightarrow 14
6285(1) ^b	0.08(3)	6285 \rightarrow 0
6314(1) ^b	0.17(3)	6314 \rightarrow 0
6338.05(23) ^b	0.60(3)	6353 \rightarrow 14
6345(1) ^b	0.06(3)	6482 \rightarrow 136
6346(1) ^b	0.08(3)	6346 \rightarrow 0
6365(1) ^b	0.16(8)	6365 \rightarrow 0
6380.63(8) ^b	7.18(13)	7646 \rightarrow 1265
6393.7(5) ^b	0.12(4)	6408 \rightarrow 14
6407.4(5) ^b	0.20(4)	6408 \rightarrow 0
6501.1(6) ^b	0.18(5)	6516 \rightarrow 14

TABLE II. (Continued.)

E_γ (keV)	I_γ^a	Placement (initial \rightarrow final)
6610(1) ^b	0.08(3)	6624 \rightarrow 14
6652(1) ^b	0.13(3)	6652 \rightarrow 0
6661(1) ^b	0.14(3)	6676 \rightarrow 14
6701.4(5)	0.12(4)	6837 \rightarrow 136
6710(1) ^b	0.12(6)	6725 \rightarrow 14
6731(1) ^b	0.24(4)	6746 \rightarrow 14
6753.5(5) ^b	0.06(2)	7120 \rightarrow 367
6764(1) ^b	0.09(3)	6778 \rightarrow 14
6837(1) ^b	0.06(3)	6837 \rightarrow 0
6939(1) ^b	0.47(15)	7646 \rightarrow 706
7278.76(19) ^b	48(3)	7646 \rightarrow 367
7306.5(6) ^b	0.32(7)	7321 \rightarrow 14
7312.7(9) ^c	0.22(8)	7313 \rightarrow 0
7554.2(5) ^c	0.13(5)	7555 \rightarrow 0
7631.06(8) ^b	228(4)	7646 \rightarrow 14
7645.48(8) ^b	200(3)	7646 \rightarrow 0

^aRelative intensity. For multiply placed transitions the singles γ -ray intensity has been divided on the basis of intensity balance and coincidence data. Multiply by 0.1190(7) for transition probability per 100 neutron captures, P_γ (%).

^bTransition confirmed by coincidence data.

^cTransition placed by energy sums.

^dTransition adopted from ENSDF [12].

2920.60-keV levels were not seen in either the singles or coincidence measurements. The method of placement of each γ ray in the decay scheme is noted in Tables I and II.

Data for 97 levels and the neutron capture state in ^{57}Fe are summarized in Table III. Level energies were determined by a least-squares fit of the recoil-corrected γ -ray energies to the level scheme. The spins and parities of the ^{57}Fe levels in Table III are discussed in the ENSDF evaluation [12] and are based on all experimental reaction and decay data populating ^{57}Fe , including the results discussed here. The intensity balance reported in Table III has been corrected for internal conversion including internal pair conversion (IPC) [13] which varies 0.13–0.26% for $E1$ and $M1$ transitions with energies of 3.0–7.6 MeV.

We found that ≈ 33 levels assigned to ^{57}Fe by Vennink *et al.* [6] could not be confirmed by this work, while an approximately equal number of new levels were added to the ^{57}Fe level scheme. Many of the new levels involved different placements of γ rays first observed by Vennink *et al.*, demonstrating the fallibility of relying on energy sums for γ -ray placement and the necessity of coincidence data for reliable construction of a level scheme.

A. Intensity balance

The γ -ray transition intensities have been corrected for a small contribution from internal conversion, calculated with the BRICC code [13], assuming either experimentally determined multipolarities or $M1$, $E1$, or $E2$ depending on the initial and final level spins and parities. When the spin or parity of the initial or final levels was unknown, $E1$ multipolarity

TABLE III. Level energies, J^π , and intensity balance per 100 neutron captures feeding/deexciting levels in ^{57}Fe .

E_{level} (keV)	J^π	P_γ (in)	P_γ (out)	P_γ (in-out)
0.0	1/2 ⁻	101.0(10) ^a		
14.399(7)	3/2 ⁻	62.4(9) ^a	62.4(9) ^a	0.0(17)
136.444(10)	5/2 ⁻	4.67(4)	4.93(7)	-0.26(8)
366.747(9)	3/2 ⁻	15.2(4)	15.26(17)	0.0(4)
706.418(12)	5/2 ⁻	6.89(8)	7.07(8)	-0.19(12)
1007.22(5)	7/2 ⁻	0.227(14)	0.230(6)	-0.003(17)
1198.39(24)	9/2 ⁻	0.008(4)	0.0067(15)	0.002(4)
1265.009(15)	1/2 ⁻	2.256(23)	2.49(4)	-0.24(4)
1357.20(9)	7/2 ⁻	0.386(13)	0.388(13)	-0.002(19)
1627.292(16)	3/2 ⁻	10.79(16)	10.91(4)	-0.11(16)
1725.449(15)	3/2 ⁻	10.95(19)	11.05(11)	-0.09(22)
2118.27(3)	5/2 ⁻	0.383(0)	0.391(6)	0.008(11)
2207.24(4)	5/2 ⁻	0.438(9)	0.510(7)	-0.071(11)
2504.95(3)	5/2 ⁺	0.381(9)	0.399(7)	-0.018(12)
2554.12(25)	3/2 ⁻	0.209(6)	0.290(6)	-0.081(8)
2574.069(24)	(3/2) ⁻	0.277(6)	0.276(7)	0.001(9)
2697.069(17)	1/2 ⁻	1.05(3)	1.017(14)	0.04(3)
2835.935(22)	3/2 ⁽⁺⁾	2.09(4)	2.264(21)	-0.18(4)
2920.56(7)	1/2 ⁻ , 3/2 ⁻	0.150(6)	0.145(6)	0.005(8)
2970.60(7)	3/2 ⁻	0.653(17)	0.65(3)	0.00(3)
3183.07(4)	1/2 ⁻ , 3/2 ⁻	0.587(24)	0.628(17)	-0.04(3)
3239.911(21)	1/2 ⁻	1.97(4)	2.030(25)	-0.06(4)
3298.28(8)	(1/2 ⁺ , 3/2 ⁺)	0.087(4)	0.108(5)	-0.021(7)
3371.17(4)	3/2 ⁻	0.597(11)	0.610(11)	-0.013(16)
3427.840(17)	3/2 ⁻	4.42(7)	4.47(8)	-0.05(11)
3547.43(9)	3/2 ⁻	0.076(6)	0.076(7)	0.000(9)
3660.23(25)	(5/2 ⁺)	0.091(4)	0.054(12)	0.038(13)
3791.747(19)	3/2 ⁺	1.576(25)	1.584(19)	-0.007(18)
3819.59(25)	(5/2 ⁺)	0.098(4)	0.114(6)	-0.16(7)
3948.49(16)	(5/2 ⁺)	0.033(4)	0.033(6)	0.000(7)
3981.66(5)	3/2 ⁻	0.184(6)	0.219(25)	-0.04(3)
4140.01(15)	5/2 ⁺	0.042(7)	0.041(4)	0.002(8)
4159.20(3)	1/2, 3/2	0.505(11)	0.486(17)	0.019(20)
4209.355(25)	3/2 ⁻	2.07(4)	2.003(18)	0.07(4)
4248.78(7)	5/2 ⁽⁺⁾	0.044(5)	0.039(6)	0.005(8)
4378.54(4)	3/2 ⁻	1.59(3)	1.514(18)	0.07(3)
4460.24(3)	(1/2 ⁻ , 3/2 ⁻)	0.887(17)	0.87(4)	0.02(4)
4474.0(10)	(5/2 ⁺)	0.026(13)	0.026(13)	0.000(18)
4547.79(7)	1/2 ⁻ , 3/2	0.064(6)	0.081(12)	-0.017(13)
4575.87(17)	1/2 ⁻ , 3/2	0.106(4)	0.080(7)	0.026(8)
4692.13(5)	(3/2 ⁺)	0.382(15)	0.327(16)	0.055(22)
4772.62(4)	(3/2 ⁺)	0.451(8)	0.440(21)	0.011(22)
4825.5(3)	1/2 ⁺ , 3/2 ⁺	0.12(4)	0.126(12)	-0.01(4)
4832.30(8)	3/2 ⁻	0.126(6)	0.086(6)	0.040(9)
4845.47(6)	1/2, 3/2	0.103(5)	0.062(4)	0.041(7)
4922.9(3)	1/2 ⁻ , 3/2	0.040(13)	0.071(12)	-0.031(18)
4963.6(3)	(5/2 ⁺)	0.030(10)	0.030(14)	0.000(17)
5046.00(12)	(1/2)	0.084(16)	0.015(7)	0.069(17)
5083.63(10)	1/2 ⁺ , 3/2	0.058(5)	0.059(7)	-0.001(8)
5164.0(10)	1/2 ⁺	0.019(10)	0.019(10)	0.000(14)
5221.75(25)	1/2, 3/2	0.061(4)	0.062(4)	-0.001(6)
5238.34(6)	1/2 ⁻ , 3/2	0.171(5)	0.147(9)	0.024(11)
5260.31(3)	1/2, 3/2	0.157(4)	0.213(7)	-0.056(7)
5308.08(6)	(3/2 ⁻)	0.090(4)	0.082(8)	0.008(9)
5428.82(10)	3/2 ⁺	0.054(3)	0.054(6)	0.000(7)
5482.0(7)	1/2, 3/2	0.0036(18)	0.037(18)	-0.033(18)

TABLE III. (*Continued.*)

E_{level} (keV)	J^π	P_γ (in)	P_γ (out)	P_γ (in-out)
5488.37(25)	1/2,3/2	0.0208(23)	0.020(4)	0.001(4)
5491.55(10)	1/2,3/2	0.050(3)	0.059(6)	-0.009(7)
5494.53(4)	1/2 ⁻ ,3/2	0.245(5)	0.192(10)	0.053(11)
5521.8(3)	1/2 ⁺	0.0102(21)	0.011(4)	-0.001(4)
5629.23(7)	3/2	0.068(3)	0.058(7)	0.010(7)
5689.40(14)	3/2	0.064(4)	0.029(5)	0.035(6)
5713.23(18)	(1/2 ⁺)	0.0149(24)	0.008(7)	0.007(8)
5790.1(3)	1/2,3/2	0.080(3)	0.101(25)	0.021(25)
5886.10(4)	1/2 ⁻ ,3/2	0.105(3)	0.109(12)	-0.004(12)
5893.53(9)	1/2,3/2	0.0271(19)	0.018(3)	0.009(4)
5923.51(4)	1/2 ⁻ ,3/2	0.463(11)	0.45(6)	0.01(6)
5974.67(7)	(3/2 ⁺)	0.067(3)	0.021(6)	0.046(7)
6012.8(3)	1/2,3/2	0.012(3)	0.027(7)	-0.015(8)
6029.36(25)	3/2 ⁺	0.0136(19)	0.014(4)	0.000(4)
6037.4(3)	1/2,3/2	0.0162(20)	0.019(10)	-0.003(10)
6040.3(3)	1/2,3/2	0.0245(21)	0.045(7)	-0.021(7)
6061.47(15)	1/2,3/2	0.101(4)	0.101(8)	0.000(9)
6074.7(3)	1/2,3/2	0.061(3)	0.065(16)	-0.004(16)
6117.02(12)	1/2 ⁺ ,3/2	0.0199(19)	0.052(9)	-0.032(9)
6159.55(13)	3/2 ⁻	0.070(4)	0.073(8)	-0.003(9)
6215.42(12)	1/2 ⁺	0.0484(23)	0.048(8)	0.000(8)
6284.6(6)	1/2,3/2	0.0094(24)	0.0010(4)	-0.0006(24)
6313.86(9)	1/2,3/2	0.0377(20)	0.052(6)	-0.015(6)
6346.11(19)	1/2,3/2	0.0131(17)	0.010(4)	-0.004(4)
6352.85(5)	1/2,3/2	0.130(4)	0.146(6)	-0.016(7)
6364.87(5)	3/2 ⁺	0.101(3)	0.077(11)	0.024(11)
6408.36(17)	3/2 ⁺	0.104(7)	0.129(9)	-0.025(12)
6481.0(10)	1/2,3/2	0.007(4)	0.007(4)	0.000(6) ^c
6515.68(7)	3/2 ⁺	0.0257(19)	0.021(6)	-0.004(6)
6624.2(3)	1/2,3/2	0.0092(14)	0.010(4)	-0.001(4)
6651.7(3)	1/2 ⁺ ,3/2	0.023(4)	0.026(5)	-0.003(6)
6675.70(25)	3/2 ⁺	0.0171(23)	0.017(4)	0.000(4)
6724.0(10)	1/2,3/2	0.014(7)	0.014(7)	0.000(1) ^c
6745.50(7)	1/2,3/2	0.0386(24)	0.048(6)	-0.009(6)
6778.4(3)	1/2,3/2	0.0102(23)	0.011(4)	-0.001(4)
6790.29(19)	1/2,3/2	0.0113(18)	0.008(6)	-0.003(6)
6837.34(11)	1/2 ⁻ ,3/2	0.055(18)	0.054(7)	0.000(19) ^c
7120.3(3)	1/2,3/2	0.0075(14)	0.0071(24)	0.000(3) ^c
7313.2(8)	1/2,3/2	0.026(10) ^c	0.026(10)	0.000(14) ^c
7321.27(13)	1/2,3/2	0.063(24) ^c	0.063(24)	0.00(3) ^c
7554.4(3)	1/2,3/2	0.015(6) ^c	0.015(6)	0.000(9) ^c
7646.183(18) ^b	1/2 ⁺		99.5(8)	

^aCorrected for unobserved statistical feeding as described in the text.

^bNeutron capture energy.

^cPrimary γ -ray populating level was not observed. The intensity is from the intensity balance.

was assumed. The total observed primary transition intensity depopulating the capture state is $98.5 \pm 1.3\%$ of that seen feeding the ground and 14-keV states, indicating that the level scheme is nearly complete. The intensity of the 23 unplaced transitions is only 0.14% of the total placed transition intensity.

To estimate the unobserved transition intensity contribution to the ^{57}Fe decay scheme, we have plotted the intensity per 100 neutron captures, $P_\gamma(\%)$, from the renormalized intensities in Tables I and II (see footnote "a"), for all γ rays, primary γ

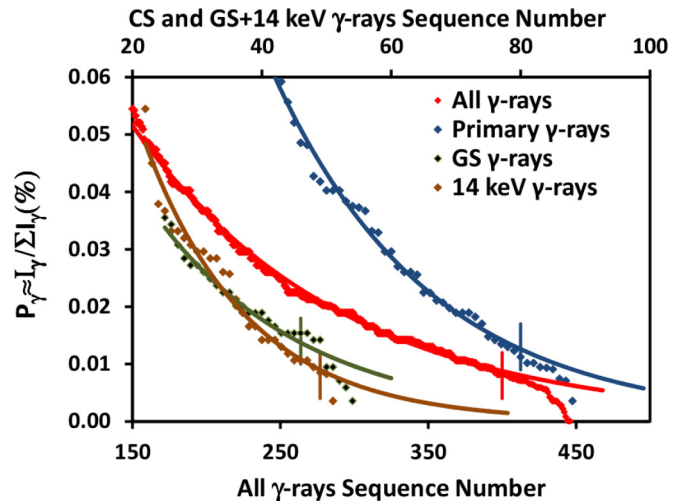


FIG. 1. Plot of ^{57}Fe transition probabilities, $P_\gamma(\%)$, ordered by their decreasing value, for all, primary, ground state (GS), and 14-keV level feeding γ rays. The solid lines through each plot represent an exponential fit through the data below N_{cut} , indicated by the vertical lines in each curve. Extrapolation of the fit to higher γ -ray numbers gives an estimate of the unobserved feeding. The parameters of each exponential fit are given in Table IV.

rays, and γ rays feeding the GS and 14-keV levels in order of decreasing $P_\gamma(\%)$ value in Fig. 1. Each of these $P_\gamma(\%)$ distributions can be fit to a simple exponential. The fitting parameters for these four exponential fits are summarized in Table IV. In each fit we have ignored both the most intense γ rays, which deviate from an exponential fit, and the least intense $\approx 10\%$ transitions, above a cutoff N_{cut} . The weakest transitions may not all be observed, which is consistent with Fig. 1 where, above N_{cut} , the $P_\gamma(\%)$ values begin to fall below the exponential trend. Integrating the exponential fits from N_{cut} to a maximum number of transitions, N_{max} gives an estimate of the total missing transition probability. For the primary, GS, and 14-keV level transitions we assume $N_{\text{max}} = 330$,

TABLE IV. The $P_\gamma(\%)$ distribution for all, primary (CS), ground state (GS), and 14-keV level feeding γ rays have been fit to an exponential defined as $P_\gamma(\%) = ae^{-bN}$ where N is the γ -ray number in decreasing intensity. N_γ is the total number of transitions observed in each category. The unobserved contribution was calculated by integrating the exponential from a cutoff transition number, N_{cut} , to a maximum number of transitions, N_{max} , and subtracting the intensity of transitions experimentally observed above N_{cut} .

Parameters	N_γ	N_{cut}	$\sum_{N_{\text{cut}}}^{N_\gamma} P_\gamma(\%)$	$\sum_{N_{\text{cut}}}^{N_{\text{max}}} P_\gamma(\%)$	netcalc-expt ^b			
a	b		expt	calc	netcalc ^a			
All	0.015	0.071	448	397	0.28	0.37	1.27	0.99
CS	0.35	0.041	89	80	0.08	0.11	0.32	0.25
GS	0.12	0.049	55	42	0.08	0.11	0.32	0.18
14	0.098	0.042	51	46	0.040	0.058	0.33	0.29

^a $N_{\text{max}} = 330$ for GS, 14 keV, and CS transitions, and 1000 for all transitions.

^bTotal unobserved percent transition probability.

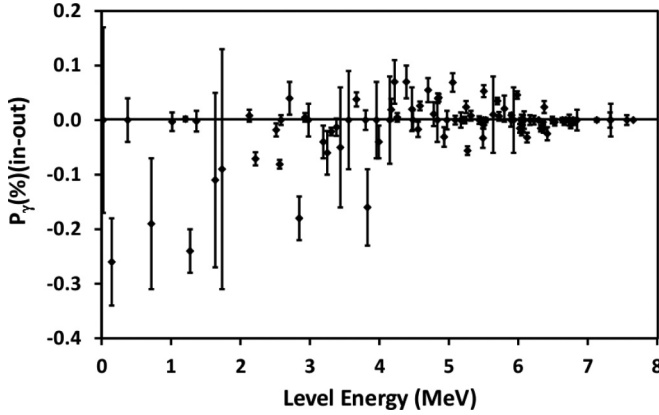


FIG. 2. The $P_\gamma(\%)$ balance populating/depopping levels in ^{57}Fe following thermal neutron capture.

the number of levels that can be fed by a dipole transition according to the constant temperature (CT) model prediction, and we arbitrarily limit the total number of transitions to $N_{\text{max}} = 1000$. The integral is not very sensitive to the choice of N_{max} because the transition probability is observed to fall off very rapidly with transition number. The theoretical justification for this estimate is discussed below.

The calculated missing transition probabilities are summarized in Table IV. For the total observed γ -ray spectrum we estimate that $\approx 1\%$ of the total transition probability is missing. This is remarkably consistent with the total observed γ -ray energy production, $\sum P_\gamma(\%)E_\gamma/(100 \times S_n) = 0.989 \pm 0.014$, where S_n is the neutron separation energy. We calculate the total missing primary γ -ray transition probability $\Delta P_\gamma(\%)(\text{CS}) = 0.25\%$. For γ rays feeding the GS + 14 keV levels the missing transition probability is $\Delta P_\gamma(\%)(\text{GS} + 14) = 0.47\%$. This missing transition probability is consistent with the variations in the transition probability balance shown in Fig. 2 and lower than the statistical uncertainty in the total primary and GS + 14 keV level feedings. For the $^{56}\text{Fe}(n,\gamma)$ decay scheme the average γ -ray multiplicity per neutron capture is $M_\gamma = \sum P_\gamma(\%)/100 = 1.83$ and the total multiplicity, including internal conversion, is $M_{\gamma+e} = \sum P_{\gamma+e}(\%)/100 = 2.39$.

The γ -ray intensities in Tables I and II are normalized relative to 100 for the 352.347-keV γ -ray and can be renormalized to percent transition probabilities, $P_\gamma(\%)$, by the factor 0.1190 ± 0.0007 , assuming that the sum of the observed GS + 14 keV level feedings and CS deexcitation transition probabilities, $P_\gamma(\text{GS} + 14 + \text{CS})\% = 200$, after correcting for the missing transition probabilities as described above. The transition probability balance through all proposed levels in ^{57}Fe is shown in Table III and summarized in Fig. 2. The decay scheme is very well balanced, with discrepancies of $\Delta P_\gamma(\%) \lesssim 0.3\%$ through all levels.

B. $^{56}\text{Fe}(n,\gamma)$ cross section

Two independent internal calibrations of the $^{56}\text{Fe}(n,\gamma)^{57}\text{Fe}$ γ -ray cross sections were performed with iron(III) acetylacetonate ($\text{C}_{15}\text{H}_{21}\text{FeO}_6$) and iron pyrite

(FeS_2) targets. The iron(III) acetylacetonate target, provided by Sigma-Aldrich, was certified as 99.9% pure on a trace metals basis, but the purity of the Fe(III) oxidation state was not explicitly given. Iron(III) acetylacetonate is 15.812(2)% Fe by weight; however, the certified Fe content was 16.0(2)%, which is consistent with the target containing $< 6.1\%$ iron(II) acetylacetonate ($\text{C}_{10}\text{H}_{14}\text{FeO}_4$). This suggests a target H/Fe ratio of 20.78 ± 0.22 . Using the 2223.2-keV γ ray from the $^1\text{H}(n,\gamma)$ reaction, assuming $\sigma_\gamma(2223) = 0.3325(7)$ b [14], we determined the 352.3-keV γ -ray cross section to be $0.2844(19)$ b.

Iron pyrite occurs only in the Fe(II) oxidation state since the Fe(III) sulfide is unstable and does not appear in nature. From our prompt γ -ray measurements on the pyrite target we set a limit of $< 0.5\%$ for sulfide impurities. Using the 841-keV γ ray from the $^{32}\text{S}(n,\gamma)$ reaction, assuming $\sigma_\gamma(841) = 0.353(2)$ b [15], we determined $\sigma_\gamma(352) = 0.2858(26)$ b. The weighted average of these two measurements is $\sigma_\gamma(352) = 0.2849(15)$ b. This value together with $P_\gamma(352) = 11.90 \pm 0.07\%$ from the level scheme normalization gives the $^{56}\text{Fe}(n,\gamma)$ total radiative cross section as $\sigma_0 = 2.394(19)$ b. This measured cross section is independent of the neutron flux for a homogenous target since it is only dependent on the ratio of ^1H and ^{32}S standardization cross sections to the 352-keV γ -ray transition probability. The guided neutron beam energy used in these measurements is subthermal energy so no correction was necessary for epithermal contributions to the measured γ -ray cross sections.

Only three measurements of $^{56}\text{Fe}(n,\gamma)$ were found in the literature, 2.65(8) b by Pomerance [16] based on the pile oscillator method, which has been renormalized to the modern $^{197}\text{Au}(n,\gamma)$ cross section calibration standard [17], 2.57(14) b by Shcherbokov *et al.* [18], based on a time-of-flight measurement, and 2.51(4) b [15] by Revay and Molnár based on an earlier prompt γ -ray measurement. The recommended cross section from Mughabghab [17] is 2.59(14) b. All previous values are significantly higher than our measurement, which has a considerably smaller uncertainty.

C. ^{57}Fe neutron separation energy

A weighted least-squares fit of the recoil-corrected γ -ray energies to obtain the level energies in ^{57}Fe determined the neutron separation energy for the capture state to be 7646.183(18) keV. This value is slightly higher than the adopted value of 7646.08(4) keV from the 2013 mass evaluation by Wang *et al.* [19].

IV. STATISTICAL MODEL TESTS

The transition probabilities observed in this work can be compared with calculated values using the Monte Carlo computer code DICEBOX [20]. DICEBOX is based on the generalization of the extreme statistical model embodying Bohr's idea of a compound nucleus [21]. We have simulated the decay of the ^{57}Fe capture state with several photon strength function models. Here we show results only for simulations with a combination of the Kadmenskij-Markushev-Furman (KMF) $E1$ photon strength function (PSF) [22] and the

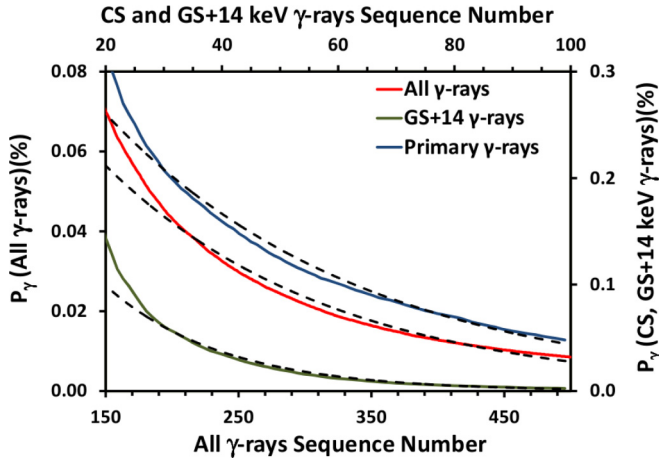


FIG. 3. Plot of simulated ^{57}Fe transition probabilities, $P_\gamma(\%)$, ordered by decreasing value for all, primary, and GS + 14 keV level feeding γ rays and averaged over 40 realizations with model A. The dashed black lines through each plot are an exponential fit through the predictions.

single-particle (SP) model [23] $M1$ PSF, labeled model A, and a PSF model based on the Oslo data [24] with an “upbend” of $M1$ origin, labeled model B. Levels in both models were generated using the constant temperature (CT) level density (LD) model [25]. The spins and parities of levels below an excitation energy $E_{\text{crit}} = 2.56$ MeV, where the level scheme is believed to be complete, are from the recent ^{57}Fe ENSDF evaluation [12], while the γ -ray transition probabilities deexciting levels below E_{crit} and primary transition probabilities feeding these levels are taken from this work. Above E_{crit} , individual levels were generated using the LD model, and transition probabilities were obtained using Monte Carlo method assuming the Porter-Thomas (PT) distribution [26] around expectation values given by the PSF model. Random fluctuations can produce an infinite number of different artificial sets of levels and decay intensities called nuclear realizations. Typically 40 different nuclear realizations were simulated for each combination of PSFs and LD models. The number of cascades in each realization was 10^6 .

In Fig. 3 we have plotted ordered transition probabilities, averaged over 40 nuclear realizations, for all γ rays, primary γ rays, and γ rays feeding the GS + 14 keV levels, as predicted by model A. Each set of transitions can reasonably be fit with an exponential, as we observed in Fig. 1 and discussed in Sec. III A. Predictions for individual nuclear realizations significantly vary in magnitude, some agreeing with experiment. However, the shapes of predictions are similar for all nuclear realizations. Predictions with model B show a similar exponential trend although the absolute magnitude does not agree as well with experiment. These calculations reinforce the validity of our method for estimating the missing transition intensity.

Simulations can also be used to investigate the intensity balance through levels below E_{crit} . We can compare the simulated feeding of these levels from levels above E_{crit} , excluding the capture state that is taken from experiment,

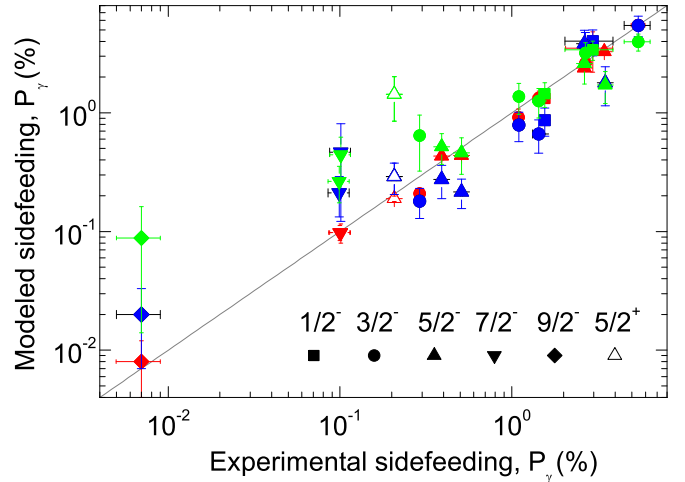


FIG. 4. Simulated vs experimental side-feeding transition probabilities, $P_\gamma(\%)$. The modeled side-feeding corresponds to the predicted feeding from levels above E_{crit} except for the capture state. Experimental side-feeding corresponds to the difference between the intensity deexciting levels below E_{crit} , minus the capture state feeding, and the feeding intensity from levels below E_{crit} . Calculations were done using models A (blue markers) and B (green markers) that are described in the text. The observed side-feeding is shown (red markers) for comparison.

with the missing experimental feeding from levels below E_{crit} . The missing experimental feeding is defined as the difference between the intensity deexciting a level and the intensity populating that level from levels below E_{crit} and from the capture state. We call these quantities the modeled and experimental side-feedings, which should ideally be equal. The side-feeding comparison, expressed as $P_\gamma(\%)$, for both A and B models is shown in Fig. 4. Modest agreement between the experimental and modeled side-feedings indicates that the statistical model calculations using available models of the PSF and level density are adequate in ^{57}Fe . There is a general trend for levels with higher experimental side-feeding to have higher simulated side-feedings, indicating that the statistical model can reasonably predict the population of low-lying levels even for light nuclei like ^{57}Fe . A better description of experimental data is obtained with model B except for the side-feeding of the $5/2^+$ state. The $5/2^+$ state is the lowest excited positive parity state, suggesting that discrepancies may arise from the LD model, which does not consider the parity distribution. Similar side-feeding agreement was also obtained with the other tested PSF models. The observed side-feeding, defined as above but using the experimental population from levels above E_{crit} instead of the simulated feedings, is also shown in Fig. 4. This side-feeding is well balanced, showing that the experimental side-feeding is well determined and simulated side-feeding discrepancies are largely due to inadequacies in the models.

There are more variables that could be used for testing various PSF and LD models within statistical model calculations and possibly the validity of the statistical model itself. However, such an analysis goes beyond the scope of this paper and will be published separately.

V. CONCLUSIONS

The $^{56}\text{Fe}(n,\gamma)$ reaction has been investigated using cold neutron beams and γ -ray singles and coincidence measurements. A detailed ^{57}Fe capture state decay scheme has been constructed where $\approx 99\%$ of the γ -ray transition intensity has been placed. Approximately 33 previously adopted levels in ^{57}Fe could not be confirmed in this work while a comparable number of new levels were added. This improvement is largely the result of our coincidence data which was not available in earlier work. Internal standardization of the measured intensities in the singles spectrum with γ -ray cross section standards has determined the ^{57}Fe total radiative thermal neutron capture cross section as $\sigma_0 = 2.394 \pm 0.019$ b. This cross section includes a small correction for unobserved continuum transitions. The experimental population of low-lying levels, below $E_{\text{crit}} = 2.56$ MeV, has been compared to statistical model calculations with modest agreement.

ACKNOWLEDGMENTS

This work was performed under the auspices of the US Department of Energy by the University of California, supported by the Director, Office of Science, Office of Basic Energy Sciences, of the US Department of Energy at Lawrence Berkeley National Laboratory under Contract No. DE-AC02-05CH11231. Support was also provided by Grant No. 13-07117S of the Czech Science Foundation and by NAP-VENEUS Contract No. OMF0-00184/2006 of Hungary. The $\gamma\gamma$ coincidence experiment was carried out at the CANAM infrastructure of the NPI ASCR Řež, supported by the Ministry of Education, Youth and Sports (Project No. LM2011019). The enriched ^{56}Fe target was provided by Dr. Frank Gunsing, CERN, and obtained on loan from the Instituto de Fisica Corpuscular, University of Valencia, courtesy of J. L. Tain.

-
- [1] T. Belgya, Z. Révay, I. H. B. Fazekas, L. Dabolcsi, G. Molnár, J. O. Z. Kis, and G. Kaszás, in *Proceedings of the 9th International Symposium on Capture Gamma-Ray Spectroscopy and Related Topics*, Budapest, Hungary, October 8–12, 1996, edited by G. Molnár, T. Belgya, and Zs. Révay (Springer-Verlag, Berlin, 1997), p. 826.
- [2] Z. Révay, T. Belgya, Z. Kasztovszky, J. Weil, and G. Molnár, *Nucl. Instrum. Methods Phys. Res., Sect. B* **213**, 385 (2004).
- [3] R. B. Firestone, H. D. Choi, R. M. Lindstrom, G. L. Molnár, S. F. Mughabghab, R. Paviotti-Corcuera, Z. Révay, V. Zerkin, and C. M. Zhou, *Database of Prompt Gamma Rays from Slow Neutron Capture for Elemental Analysis*, STI/PUB/1263 (IAEA, Vienna, 2007).
- [4] *Handbook of Prompt Gamma Activations Analysis with Neutron Beams*, edited by G. Molnár (Kluwer Academic, Boston, 2004).
- [5] M. Kostal, J. Milcak, V. Rypar, V. Juricek, M. Svadlenkova, A. Kolros, and B. Jansky, *Nucl. Data Sheets* **118**, 561 (2014).
- [6] R. Vennink, J. Kopecky, P. Endt, and P. Glaudemans, *Nucl. Phys. A* **344**, 421 (1980).
- [7] F. Bečvář, J. Honzátko, M. Krtička, S. Pasic, G. Rusev, and I. Tomandl, *Nucl. Instrum. Methods Phys. Res., Sect. B* **261**, 930 (2007).
- [8] G. Molnár, Z. Révay, and T. Belgya, *Nucl. Instrum. Methods Phys. Res., Sect. A* **489**, 140 (2002).
- [9] B. Fazekas, J. Óstór, Z. Kis, G. Molnár, and A. Simonits, in *Proceedings of the 9th International Symposium on Capture Gamma-Ray Spectroscopy and Related Topics*, Budapest, Hungary, October 8–12, 1996, edited by G. Molnár, T. Belgya, and Zs. Révay (Springer-Verlag, Berlin, 1997), p. 774.
- [10] K. Rosman and P. Taylor, *Pure Appl. Chem.* **70**, 217 (1998).
- [11] J. Honzátko, K. Konečný, I. Tomandl, J. Vacík, F. Bečvář, and P. Cejnar, *Nucl. Instrum. Methods Phys. Res., Sect. A* **376**, 434 (1996).
- [12] A. Negret, R. Firestone, and B. Singh, *Nucl. Data Sheets* (to be published).
- [13] T. Kibédi, T. Burrows, M. Trzhaskovskaya, P. Davidson, and J. C. W. Nestor, *Nucl. Instrum. Methods Phys. Res., Sect. A* **589**, 202 (2008).
- [14] R. B. Firestone and Z. Révay, *Phys. Rev. C* **93**, 044311 (2016).
- [15] Z. Révay and G. Molnár, *Radiochim. Acta* **91**, 361 (2003).
- [16] H. Pomerance, *Phys. Rev.* **88**, 412 (1952).
- [17] S. Mughabghab, *Atlas of Neutron Resonances*, 5th ed. (Elsevier, New York, 2006).
- [18] O. Shcherbakov, A. Stupak, and A. Glukhovec, *Jadernye Konstanty* **25**, 51 (1977).
- [19] M. Wang, G. Audi, A. Wapstra, F. Kondev, F. MacCormick, X. Xu, and B. Pfeiffer, *Chin. Phys. C* **36**, 1603 (2012).
- [20] F. Bečvář, *Nucl. Instrum. Methods Phys. Res., Sect. A* **417**, 434 (1998).
- [21] N. Bohr, *Nature (London)* **137**, 344 (1936).
- [22] S. Kadenskij, V. P. Markushev, and V. I. Furman, *Sov. J. Nucl. Phys.* **37**, 165 (1983).
- [23] J. Blatt and V. Weisskopf, *Theoretical Nuclear Physics* (John Wiley and Sons, New York, 1952).
- [24] M. Guttormsen, A. Larsen, J. Rekstad, S. Siem, N. Syed, A. Schiller, and A. Voinov, *PoS PSF07*, 003 (2007).
- [25] A. Gilbert and A. Cameron, *Can. J. Phys.* **43**, 1446 (1965).
- [26] C. Porter and R. Thomas, *Phys. Rev.* **104**, 483 (1956).